Radiation Protection Dosimetry (2022), Vol. 198, No. 16, pp. 1230–1237
Advance Access publication 22 July 2022
https://doi.org/10.1093/rpd/ncac161

EFFECT OF DIFFERENT SOLVENTS ON THE OPTICALLY STIMULATED LUMINESCENCE SIGNAL FROM MgB_4O_7:Ce,Li-LOADED POLYMER FILMS

Caroline C. Santos [1,*], João V.B. Valença [2], Francesco d'Errico[3,4], Rogério Machado[1], Linda V.E. Caldas[5] and Susana O. Souza[1]
[1]Physics Department, Federal University of Sergipe (DFI/UFS), São Cristóvão, SE, Brazil.
[2]DECESA, Federal University of Health Sciences of Porto Alegre (UFCSPA), Porto Alegre, RS, Brazil.
[3]Scuola di Ingegneria, Università di Pisa (UNIPI), Pisa, Italy.
[4]School of Medicine, Yale University (YALE), New Haven, CT USA.
[5]Nuclear and Energy Research Institute (IPEN), São Paulo, SP, Brazil.

*Corresponding author: scastrocaroline@gmail.com

Received 9 April 2022; revised 31 May 2022; editorial decision 28 June 2022; accepted 28 June 2022

The detailed dose analysis at the extremities remains a challenge, without affecting operators' mobility and their tactile sense. Using films loaded with optically stimulated luminescence (OSL) crystals have been studied in order to overcome some of these challenges in 2D dosimetry. In this work, we investigated flexible polymeric films loaded with MgB_4O_7:Ce,Li to acquire a better understanding of the dependence of the dosimetric signal characteristics on the production process and the influence of using different powder grain sizes. In film production, five different solvents were used: acetone–benzene, dichloromethane, chloroform, tetrahydrofuran and formic acid. Our results indicate that acetone–benzene is the solvent mixture that less influences the signal emitted by treated crystals, in comparison with the signal emitted by the pristine crystal powder. Conversely, by using formic acid, the crystalline structure of the sample was most severely modified, leading to a drastic reduction of the emitted OSL signal. We found that the extent of the grain surface in contact with the solvent in the process is important and should be taken into consideration when choosing the proper grain size to be used.

Highlights

- **Polymeric films loaded with MgB_4O_7:Ce,Li crystals were produced using different solvents.**
- **Different effect on the OSL signal was found depending on the used solvent.**
- **Among the evaluated solvents, acetone–benzene was the one that less affected the OSL signal.**

INTRODUCTION

Ionising radiation dosimetry is an important area, considering the increasing use of ionising radiation in different fields. One dosimetric challenge is to determine complex entrance dose distributions. For example, in extremity dosimetry, a major challenge is to develop a dosemeter that allows an easy and reliable dose quantification for different parts of the hands without interfering with the handling abilities. Several studies have been performed aiming to overcome this limitation with regards to 2D dosimetry, including the promising use of polymeric films combined with light-emitting materials[1], which could generate dosimetric films so flexible that it is possible to produce gloves[2].

Some polymeric films present adequate characteristics to be used in medical applications, as well as technological innovations, and have been investigated for drug delivery[3], temporary skin replacement[4] and radiation dosimetry[5, 6]. There are several advantages in using polyvinyl chloride (PVC) to produce polymeric films, such as low production cost, high chemical resistance, impermeability to liquids and gases and transparency to visible light[7, 8].

Among several potential candidates as the OSL emitter, magnesium tetraborate doped with cerium and lithium (MgB_4O_7:Ce,Li) draws attention, especially because the host MgB_4O_7 crystalline structure has been studied for decades[9–12]. This material has been used as the matrix for several thermoluminescence dosemeters when doped/co-doped with specific ions[13, 14] and, more recently, its optically stimulated luminescence (OSL) signal has been investigated[15, 16]. MgB_4O_7:Ce,Li has been analysed with respect to its TL and OSL signals[5, 16, 17], which showed great potential for use in ionising radiation dosimetry. Among its appealing features for luminescent dosimetry, one can quote: tissue-equivalent effective atomic number, high sensitivity[12], linear response behaviour over a wide dose range[14, 18], and the

possible use as thermal neutron detector (thanks to the ^{10}B isotope). The potential use of MgB_4O_7:Ce,Li-based films for 2D dosimetry, associated with its OSL emission characteristics, was recently explored[19]. In that study, MgB_4O_7:Ce,Li was produced by combustion synthesis, whereas a Kraton™ FG1901X solution (Kraton Co.) in toluene and low molecular weight methyl polysiloxane were used for the films. Further studies on the use of MgB_4O_7:Ce,Li were warranted by the authors, due to the need to better understand processes that lead to sensitivity changes and fading of the emitted signal.

In this context, the main objective of the present work was to demonstrate the feasibility of producing a highly flexible film with PVC loaded with MgB_4O_7:Ce,Li and find the most suitable PVC solvent to produce these films. The effect of the solvents on the crystal characteristics was evaluated based on OSL signal analysis and X-ray diffraction (XRD). A first study of the effect of the solvents on different grain sizes of MgB_4O_7:Ce,Li was also performed.

MATERIALS AND METHODS

Solid-state synthesis was used to produce both the undoped and doped/co-doped varieties of magnesium tetraborate (MgB_4O_7) samples. Four different varieties of crystals were produced: pure (undoped) magnesium tetraborate (MgB_4O_7), cerium-doped magnesium tetraborate (MgB_4O_7:$Ce_{0.5\%}$) and cerium-doped magnesium tetraborate co-doped with lithium (MgB_4O_7:$Ce_{0.5\%}Li_{0.1\%}$ and MgB_4O_7:$Ce_{0.5\%}Li_{0.5\%}$). Magnesium oxide (MgO; Sigma-Aldrich, 98% purity) and boric acid (H_3BO_3; Sigma-Aldrich, 99% purity) were used to obtain the crystal matrix of MgB_4O_7. The doping process included cerium oxide (CeO_2; Sigma-Aldrich, 99% purity) and lithium carbonate (Li_2CO_3; Sigma-Aldrich, 99% purity), which were added based on the total weight. After mixing and milling stoichiometric number of reagents, the mixture was calcinated in an electric furnace (EDG-1800) for 7 h at 900 °C (coolant temperature rate of 10 °C per min). Four batches were produced; the obtained powder was sieved and separated based on the grain size: smaller than 45 μm and between 45 and 75 μm.

To confirm the crystal structure obtained, XRD was performed using samples with grain sizes smaller than 45 μm. This technique is very well established for this purpose, being the obtained peaks related to the specific constructive interference patterns that happen differently (different angles and relative intensities, for example) depending on the crystal structure, which is analysed by using a specific X-ray beam. A Bruker D8 Advance diffractometer was used for the measurements with the following settings: 40 kV/25 mA, CuK_α, scan range from 10 to 80º and steps of 4º/min. Rietveld refinement was used to determine the proportions of the crystalline phases presented in the produced samples.

When pellets were used for the analysis, they were obtained by mixing/homogenising the powder samples with Teflon (at 1:1 ratio) and pressing the mix under 50 kgf/cm^2. A thermal treatment of 350 °C for 30 min followed by 400 °C for 1 h was performed for the produced pellets. The obtained pellets had mass, diameter and thickness approximately equal to 0.04 g, 6 mm and 1 mm, respectively.

Five different types of solvents were used to investigate their influence on the OSL response of MgB_4O_7:$Ce_{0.5\%}Li_{0.5\%}$: acetone–benzene ($0.4C_3H_6O$-$0.6C_6H_6$; Neon, 99.5% purity and Sigma-Aldrich, 99.5% purity, respectively), dichloromethane (CH_2Cl_2; ISOFAR, 99.5% purity), chloroform ($CHCl_3$; Synth, 99.8% purity), tetrahydrofuran–THF (C_4H_8O; Sigma-Aldrich, 99% purity) and formic acid (CH_2O_2; Sigma-Aldrich, 99%). A well-defined amount of powder was completely immersed in each type of solvent (proportion of 1:10) and placed on agitation until the end of solvent evaporation. This procedure was performed for two crystal grain sizes: smaller than 45 μm and between 45 and 75 μm.

Highly flexible films loaded with grains of MgB_4O_7:Ce,Li can be manufactured with various techniques available to our consortium of laboratories: solvent-evaporation, pressure casting or bubble blowing of polymer blends. The polymer films produced by the casting technique are composed of a mixture of polymer, plasticiser and solvent at fairly low temperatures. The solvent-evaporation is a relatively easy technique, and it allows the rapid production of small test-samples; however, it requires a careful selection of organic solvents to avoid affecting the luminescent properties of the dispersed grains. For this work, we present the results of the films produced by the casting technique[20], like that described by Souza *et al.*[1] with regards to both the process applied and size specifications of the samples used to perform OSL measurements.

A Cs-137 gamma source was used for the irradiation that preceded the OSL analysis, and pellets were placed at 1 m distance where a dose rate of 0.32 mGy/s was delivered. During the irradiation, the pellets were inserted between 3-mm thick Polymethyl methacrylate (PMMA) plates guaranteeing electronic equilibrium. The time interval between the irradiation process and the OSL reading was no more than 20 min, and during this period the samples were kept in a dark container, in order to avoid signal losses by optical stimulation. Previous work[19] reported that fading of the signal is not significant during the first 20 min.

OSL measurements were carried out with a Risø TL/OSL DA-20 reader, using the continuous wave mode of stimulation (CW-OSL) during 60 s, with

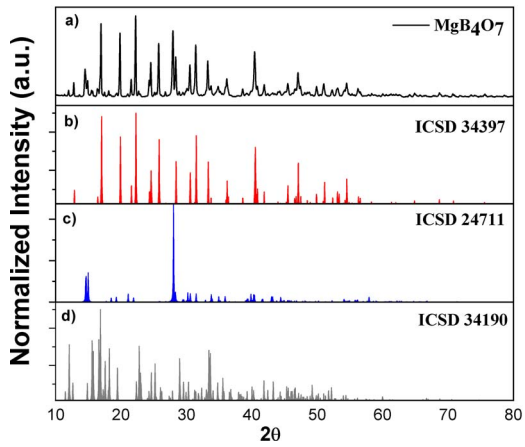

Figure 1. XRD patterns for (a) the obtained sample, (b) ICSD 34397—MgB_4O_7 of reference, (c) ICSD 24711—boric acid and (d) ICSD 34190—hydrated magnesium tetraborate.

blue LED (peak emission at 470 nm; full width at half maximum = 20 nm) as stimulation source. The reader is equipped with an EMI 9235QB Photomultiplier tube (maximum quantum efficiency at ~200 and 380 nm) for emitted light detection, and a Hoya U-340 filter (transmission between 290 and 390 nm) to discriminate stimulation light from OSL signal. Post-readout optical annealing consisted of exposing the samples to a white fluorescent lamp for 1 h, and it was used after every cycle of measurements. Dose–response curves were achieved by irradiating samples with 10, 40, 60, 80 and 100 mGy. For this analysis, the subtraction of the value recorded in the first 10 channels (2.4 s of emission) and the value from the last 10 channels was used as the parameter. All OSL analyses were performed in triplicate and the uncertainties are shown in the graphs.

Reproducibility was investigated by submitting 15 pellets and 12 small pieces of films of each batch to 5 cycles of beta ($^{90}Sr + {}^{90}Y$) irradiation (169 mGy), reading process and annealing (same configurations mentioned before). Only pellets/films that presented a variance lower than 10% were used in the analysis, the only exception being the pellets exposed to formic acid, which had a drastic change in their emission characteristics.

RESULTS AND DISCUSSION

XRD analysis (Figure 1) shows a predominant formation (70%) of the magnesium tetraborate crystalline phase (ICSD 34397). The two other detected phases, with proportions quantified by Rietveld refinement, were 11% of hydrated magnesium tetraborate (ICSD 34190) and 19% related to boric acid (ICSD 24711).

The dopant/co-dopant concentrations were chosen based on a previous work[21], which showed the optimal signal being achieved with 0.5% Li concentration in the $MgB_4O_7:Ce_{0.5\%}$ production, by using the solid-state synthesis process. The same study also showed that the addition of greater amounts of Li would not be suitable for dosimetry purposes, as it induces a reduction on the OSL emitted signal, probably due to the quenching effect. OSL measurements were carried out for all doped/co-doped pellet samples, identifying which batch presented the most intense luminescent signal for the settings applied. All samples were irradiated with a dose of 100 mGy of Cs-137 gamma rays. Figure 2a shows a considerable increase in the OSL signal when $MgB_4O_7:Ce_{0.5\%}$, was co-doped with Li. This result is consistent with previous publications[16, 17], which indicate Li acting as a charge compensator, helping Ce^{3+} to substitute Mg^{2+}, and thus contributing to the increment of OSL signal when used as co-dopant. Figure 2b exhibits the normalised OSL curves for $MgB_4O_7:Ce_{0.5\%}$, $MgB_4O_7:Ce_{0.5\%}Li_{0.1\%}$ and $MgB_4O_7:Ce_{0.5\%}Li_{0.5\%}$, from which a superposition of the co-doped samples curves is clear. Co-doping the sample with Li changed the exhibited OSL emission pattern, producing a slightly faster initial decay; however, its increment in concentration does not affect the pattern of decay.

The sample with 0.5% Li presented the most intense OSL signal (the emission with 0.1% Li doping corresponds to 46% of the intensity emitted with 0.5% Li, considering the very first 0.24 s of the measurement), and therefore, it was chosen for subsequent analysis. Using this composition, pellets were produced with different grain sizes (X): $X < 45\ \mu m$ and $45 < X < 75\ \mu m$, which were previously sieved. Figure 3a shows that the pellets made with a smaller grain size presented a more intense OSL signal. Diverging opinions on how the size of the grains affects the intensity of OSL and TL signals have been recently reported as to different materials in literature[22–24].

Figure 3b presents the intensity of the OSL signal emitted by samples with different grain sizes. To better analyse the effect of grain size on OSL measurements, the curves were divided into three integration intervals, with times of 1, 10 and 60 s using the Origin software. The intervals were chosen considering the initial drop, the part with an almost total drop in the signal, and the total curve obtained. The results show that, for a 1-s integration, the signal emitted by samples with grain sizes between 45 and 75 μm corresponds to ~82% of the signal emitted by samples with smaller grains. For longer integration times, the smaller gains are still more intense but larger grains

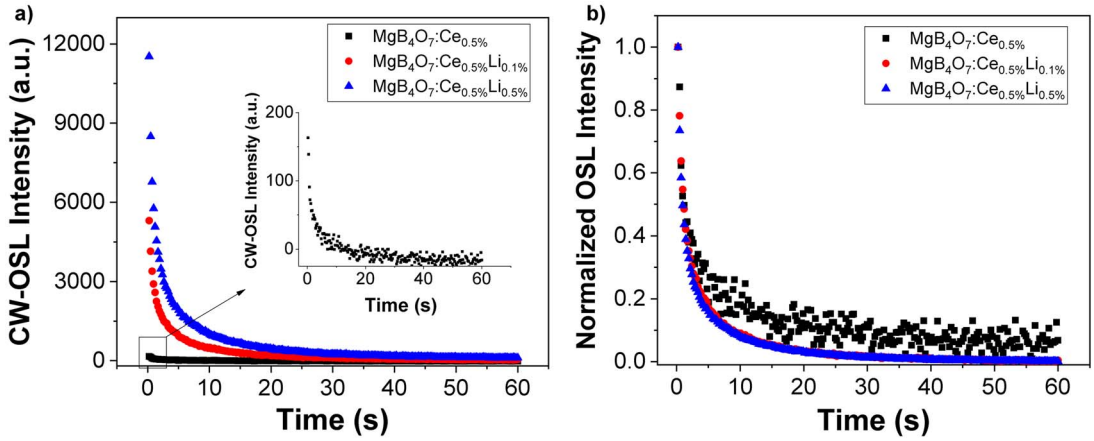

Figure 2. OSL signal emitted by (a) the $MgB_4O_7:Ce_{0.5\%}$, $MgB_4O_7:Ce_{0.5\%}Li_{0.1\%}$, and $MgB_4O_7:Ce_{0.5\%}Li_{0.5\%}$ samples after a dose of 100 mGy by using a Cs-137 gamma source (inset: zoom on the Ce-doped decay); (b) mormalised OSL signal.

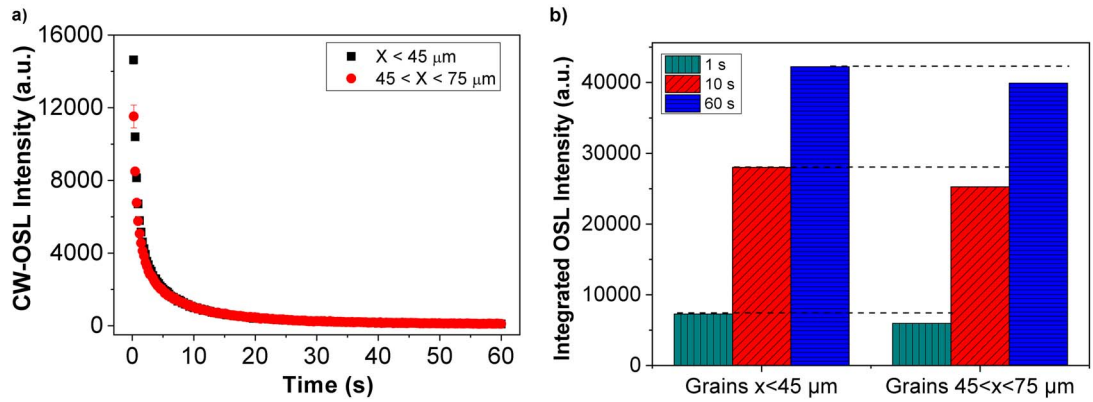

Figure 3. (a) OSL emission from pellets produced with grains of $X < 45\ \mu m$ and $45 < X < 75\ \mu m$ irradiated with gamma dose of 100 mGy. (b) Intensity of the OSL signal emitted by samples with the different sets of grains, integrated in different intervals (1, 10 and 60 s).

approach the same levels, being ~90% for 10 s and 94% for 60 s integration times.

Considering their more intense OSL emission, samples with grains smaller than 45 μm were chosen to test the effect on the OSL signal of the use of different solvents, which is an important aspect of the production process of dosimetric films. For this test, different powder samples of $MgB_4O_7:Ce_{0.5\%}Li_{0.5\%}$ were completely immersed in the different types of solvents that can be used to produce PVC films. After evaporation and complete desiccation, XRD analysis was performed on the powder, and pellets were produced using each type of sample. As shown in Figure 4a, the use of the solvents decreased the initial OSL intensity, but in different levels. Acetone–benzene had the lowest impact and reduced the OSL emission by ~20% in the first 0.24 s of stimulation (corresponding to the first channel of the light collection), and it was the option that less interfered in the original intensity. Conversely, formic acid had the highest impact on the result and the initial OSL intensity was reduced by > 98% compared with the untreated sample. The use of dichloromethane, chloroform and tetrahydrofuran reduced the signal intensity by ~26%, 29% and 49%, respectively. Except for formic acid, one can observe a similar decay pattern for the samples treated with all solvents, as seen in Figure 4b.

Figure 4c shows a different level of decrease in the OSL intensity emitted by the powder sample of $MgB_4O_7:Ce_{0.5\%}Li_{0.5\%}$ before and after treatment with different solvents. For a 1-s emission integration, the sample treated with acetone/benzene presented a signal equivalent to ~81% of the untreated sample,

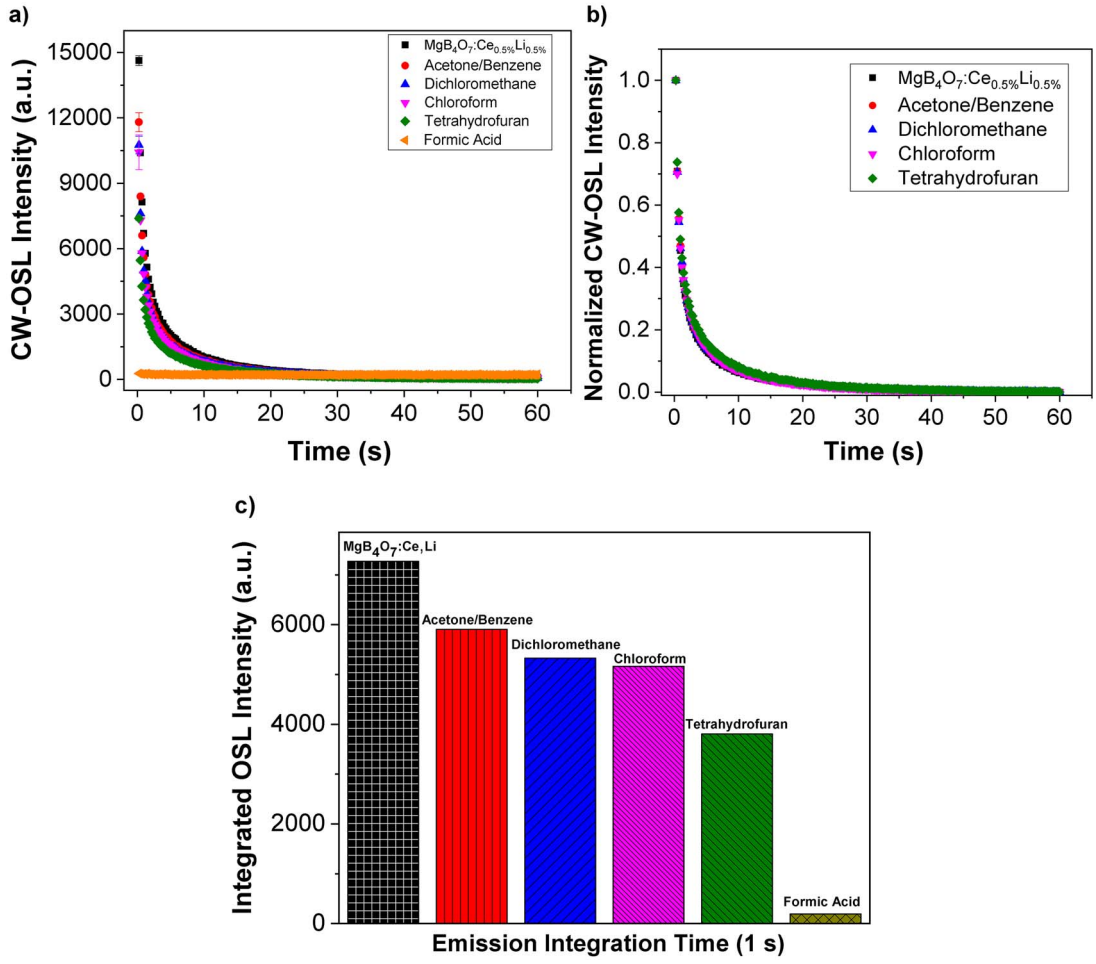

Figure 4. (a) OSL signal obtained from pure $MgB_4O_7:Ce_{0.5\%}Li_{0.5\%}$ and under influence of a previous mix with different solvents (inset: comparison of the emission in the first 0.24 s); (b) Selected normalised curves. (c) OSL signal comparison, integrated for the first second of emission, of the undoped MgB_4O_7 and this compound after mixed, and completely dried, with different solvents. All the analyses were performed after 100 mGy gamma irradiation.

which agrees with the discussion for Figure 4a. The signals emitted by the other treated samples are also lower in comparison to the untreated one, being equivalent to 73%, 71%, 52% and 2,5% for dichloromethane, chloroform, tetrahydrofuran and formic acid, respectively, when compared with the emission of the untreated samples.

All these modifications may derive from changes in the number/characteristics of traps presented in each material, resulting from different effect on the crystalline structure by the treatment with each solvent. Figure 5 shows the XRD powder pattern performed at the end of the solvent evaporation.

The use of formic acid clearly changes the diffraction pattern exhibited by the sample. The presence of new highly intense peaks as well as the disappearance of peaks or changes in their position are clear indications of the solvent effect on the crystalline structures. For the other solvents, crystalline changes are very subtle. Suggestions that modifications in crystalline structures, made by the action of solvents, can be identified by parameters as crystal volume, interplanar distances, etc., has been quoted in literature[25]. Quantitative analyses of the obtained XRD patterns were not part of the current study, but they will be performed as a next step. For the samples treated with acetone–benzene, dichloromethane, chloroform and THF, we hypothesise that changes in those parameters, as well as the impact of these changes in the energy levels introduced by the presence of the dopant

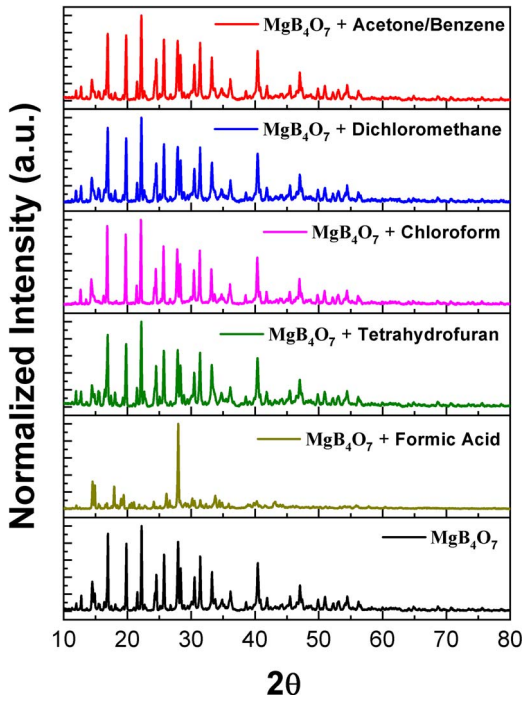

Figure 5. Powder pattern XRD of the samples treated with different types of solvents after their evaporation.

and the co-dopant, can be the explanation of the changes in the OSL intensity.

Considering its lower impact on the OSL signal, acetone/benzene was chosen as the solvent for film production with MgB_4O_7:$Ce_{0.5\%}Li_{0.5\%}$. In order to analyse the impact of the film production process on the OSL signal characteristics, PVC films were produced with both powder grain sizes: $X < 45$ μm or $45 < X < 75$ μm. As seen in Figure 6a, no OSL signal was detected from the pure polymer film, with no crystals added, when previously irradiated with a dose of 400 mGy. Figure 6b shows a more intense initial signal from the film with crystal grains of $45 < X < 75$ μm, differently from the previous discussion illustrated in Figure 3a. Factors such as the total contact surface area of the grains may play an important role in the description of the solvent impacts on the signal from different grain sizes.

Figure 6c presents a histogram comparing the OSL emission from films produced with the addition of different grain sizes. Results were obtained from time integration in 1, 10 and 60 s. A more intense signal was recorded from the bigger grain size samples, as discussed before. In this case, the emissions from the smaller grain size samples correspond to ~82% of the emission from the larger grain size samples, no matter which time interval was considered in the analysis. Figure 6d illustrates the flexibility obtained in the produced films.

Dose–response curves were obtained for films produced with each cited grain sizes and different film thicknesses (100, 300 and 400 μm). For the purpose, ^{137}Cs gamma doses ranging from 10 to 100 mGy were used, and the emission in the first 0.24 s of the measurements was evaluated. Increasing the dose was always followed by an increment in the OSL signal, as seen in Figure 7. As expected, the average value of the signal also increased with increasing thickness of the film, since a greater thickness corresponds to a larger amount of crystal powder. Clearly, in our preparation procedures, a larger amount of powder was added to the thicker films, even though it was not possible to determine exactly the amount in each case. The signal differences for a same thickness of the film, but different grains, is more clearly observed for the 300-μm film. The standard deviation bars overlap in most of the 100 and 400 μm film cases, which is a clear indication of the lack of statistical significance. Therefore, despite some indication of a greater influence of the solvents in grains with a smaller size (greater surface contact), a more detailed characterisation should be performed. While this investigation focused on the role of the PVC solvents, studies examining MgB_4O_7:$Ce_{0.5\%}Li_{0.5\%}$ fading and changes in sensitivity after several cycles of irradiation-reading-bleaching are warranted, as was also previously reported[19].

CONCLUSIONS

This work demonstrated the influence of using different solvents in the production of films loaded with crystals of MgB_4O_7:Ce,Li regarding its OSL. Of the five solvents analysed, formic acid was the one that more dramatically changed the crystalline structure, which was seen both in the XRD measurements and in the OSL signal of the samples. Using acetone–benzene proved to be less influential in the luminescence of the material, although a reduction of about 19% in the first 0.24 s of OSL signal integration is still present in comparison with untreated samples. The dose–response curves, obtained with the films produced using acetone–benzene, showed an increment in the signal as the dose increased.

Regarding the influence of the grain size in the OSL signal intensity we observed that without solvents the pellets produced with grains < 45 μm presented a more intense initial signal in comparison with grains between 45 and 75μm. The opposite occurred when analysing films loaded with different grain sizes, which is a strong indication of the more intense action of the solvents in the grains with more contact surface.

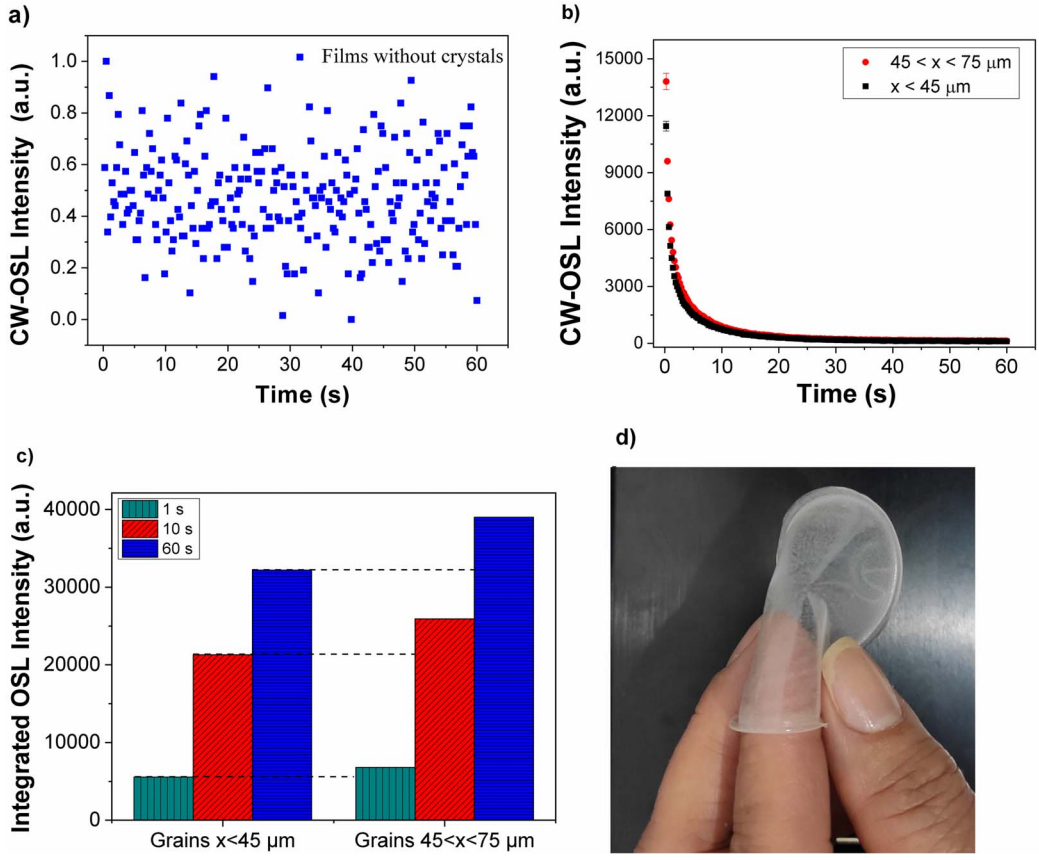

Figure 6. (a) Normalised OSL signal from the polymer film with no added crystals after irradiation of 400 mGy, (b) Comparison of the OSL signal emitted from films (400 μm thick) with different grain size crystals added after irradiation of 400 mGy (inset: comparison of the emission in the first 0.24 s). (c) Comparison of the OSL signal, emitted by the films with different sets of grains inserted, integrated into different time intervals (1 s, 10 s, and 60 s). (d) Picture of a produced film sample.

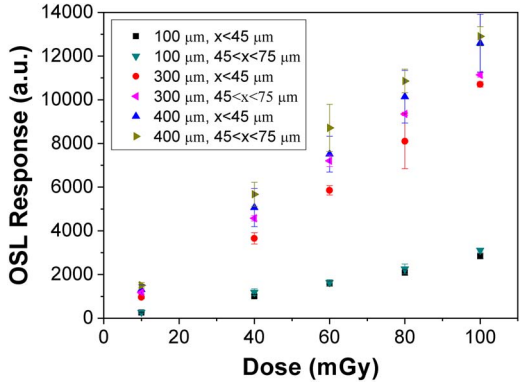

Figure 7. Dose–response curves for the films with different thicknesses (100, 300 and 400 μm) and grain sizes (x < 45 μm; 45 < x < 75 μm) added to them.

These studies support the development of crystal-loaded polymer films as a method for extremity dosimetry, which may provide accurate and reliable results while not interfering with the tactile sense of the operators.

FUNDING

Brazilian Agencies Fundação de Amparo à Pesquisa do Estado de São Paulo (Project 2018/055982-0) and Conselho Nacional de Desenvolvimento Científico e Tecnológico (Project 30/335/2016-8).

REFERENCES

1. Souza, S. O., d'Errico, F., Azimi, B., Baldassare, A., Alves, A. V. S., Valença, J. V. B., Barros, V. S. M.,

Cascone, M. G. and Lazzeri, L. *OSL films for in-vivo entrance dose measurements*. Radiat. Meas. **106**, 644–649 (2017).
2. d'Errico, F., Abegão, L., Souza, S. O., Chierici, A., Lazzeri, L., Puccini, M., Vitolo, S., Miyamoto, Y., Nanto, H. and Yamamoto, T. *Entrance surface dosimetry with radiophotoluminescent films*. Radiat. Meas. **137**, 106423 (2020).
3. Bernards, D. A. and Desai, T. A. *Nanoscale porosity in polymer films: fabrication and therapeutic applications*. Soft Matter **6**, 1621–1631 (2010).
4. Mir, M., All, M. N., Barakullah, A., Gulzar, A., Arshad, M., Fatima, S. and Asad, M. *Synthetic polymeric biomaterials for wound healing: a review*. Prog. Biomater. **7**(1), 1–21 (2018).
5. Souza, L. F., Silva, A. M. B., Antonio, P. L., Caldas, L. V. E., Souza, S. O., d'Errico, F. and Souza, D. N. *Dosimetric properties of MgB_4O_7:Dy,Li and MgB_4O_7:Ce,Li for optically stimulated luminescence applications*. Radiat. Meas. **106**, 196–199 (2017).
6. Sasiadek, E., Andrzejczak, R. and Kozicki, M. *The importance of fabric structure in the construction of 2D textile radiation dosimeters*. Radiat. Meas. **47**, 622–627 (2012).
7. Cheremisinoff, N. P. Advanced Polymer Processing Operations. (New Jersey: William Andrew) (1999).
8. Crawford, R. J. Plastic engineering, in encyclopedia of physical science and technology – polymers, 3rd edn. (U.S.A: Academic Press) pp. 457–474 (2001).
9. Paün, J., Iozsa, A. and Jipa, S. *Dosimetric characteristics of alkaline earth tetraborates radiothermoluminescent detectors*. Radiochem. Radioanal. Lett. **28**(5–6), 411–421 (1977).
10. Lakshmanan, A. R., Chandra, B., Pradhan, A. S. and Bhatt, R. C. *Development of MgB_4O_7:Dy TLD phosphor*. Radiochem. Radioanal. Lett. **37**(6), 377–382 (1979).
11. Prokić, M. *Development of highly sensitive $CaSO_4$:Dy/Tm and MgB_4O_7:Dy/Tm sintered thermoluminescent dosimeters*. Nucl. Instrum. Meth. B. **175**, 83–86 (1980).
12. Szabó, P. P., Pradhan, A. S. and Chandra, B. *Some dosimetric parameters of MgB4O7:Dy sintered pellets and CaSO4:Dy Teflon discs—a comparative study*. Inr. J. Appl. Radiat. Isor. **35**(5), 415–417 (1984).
13. Kitis, G., Polymeris, G. S., Prokic, M., Meric, N. and Pagonis, V. *Prompt isothermal decay of thermoluminescence in MgB_4O_7:Dy,Na and LiB_4O_7:Cu,In dosimeters*. Radiat. Meas. **84**, 15–25 (2016).
14. Souza, L. F., Vidal, R. M., Souza, S. O. and Souza, D. N. *Thermoluminescent dosimetric comparison for two different MgB_4O_7:Dy production routes*. Radiat. Phys. Chem. **104**, 100–103 (2014).
15. Yukihara, E. G., Milliken, D., Oliveira, L. C., Orante-Barrón, V. R., Jacobsohn, L. G. and Blair, M. W. *Systematic development of new thermoluminescence and optically stimulated luminescence materials*. J. Lumin. **133**, 203–210 (2013).
16. Yukihara, E. G., Doull, B. A., Gustafson, T., Oliveira, L. C., Kurt, K. and Milliken, E. D. *Optically stimulated luminescence of MgB_4O_7:Ce,Li for gamma and neutron dosimetry*. J. Lumin. **183**, 525–532 (2017).
17. Yukihara, E., Milliken, E. and Doull, B. *Thermally stimulated and recombination processes in MgB_4O_7 investigated by lanthanide doping*. J. Lumin. **154**, 251–259 (2014).
18. Furetta, C., Prokić, M., Salamon, R. and Kitis, G. *Dosimetric characterisation of a new production of MgB_4O_7:Dy,Na TL material*. Int. J. Appl. Radiat. Isot. **52**, 293–250 (2000).
19. Shrestha, N., Vandenbroucke, D., Leblans, P. and Yukihara, E. G. *Feasibility studies on the use of MgB4O7:Ce,Li-based films in 2D optically stimulated luminescence dosimetry*. Physics Open **5**, 100037 (2020).
20. Domenech, S. C., Bortoluzzi, J. H., Soldi, V., Franco, C. V., Gronski, W. and Radusch, H. J. *Characterization, morphology, thermal and mechanical properties of conductive polyaniline-functionalized EPDM elastomers obtained by casting*. J. Polym. Sci. B Polym. Phys. **42**, 1767–1782 (2004).
21. Souza, L. F., Novais, A. F., Antonio, P. L., Caldas, L. V. E. and Souza, D. N. *Luminescent properties of MgB_4O_7:Ce,Li to be applied in radiation dosimetry*. Radiat. Phys. Chem. **164**, 108353 (2019).
22. Yazdanmehr, M., Sadeghi, H., Tehrani, M. K., Hashemifar, S. J. and Mahdavi, M. *Effects of nanostructuring on luminescence properties of SrS:Ce,Sm phosphor: an experimental and phenomenological study*. Opt. Mater. **75**, 304–313 (2018).
23. Sahare, P. D. and Saran, M. *Particle size effects on the dosimetry characteristics of $K_3Na(SO_4)_2$:Eu TLD micro- and nanophosphors*. J. Lumin. **198**, 488–496 (2018).
24. Bhadane, M. S., Gavhane, K. H., Kulkarni, P. P., Dahiwale, S. S., Bhoraskar, V. N., More, M. A., Patil, P. S. and Dhole, S. D. *Particle size dependent TL response of CaF_2:Dy phosphor for gamma dosimetry*. J. Lumin. **223**, 117–168 (2020).
25. Horst, J. H. T., Geertman, R. M. and Rosmalen, G. M. V. *The effect of solvent on crystal morphology*. J. Cryst. Growth **230**, 277–284 (2001).